

PAPER Nr.:33



DESIGN OF NEW GENERATION ROTOR BLADE AIRFOILS  
USING NAVIER-STOKES

by

Masaaki Nakadate and Masahiro Obukata

Fuji Heavy Industries, Ltd.  
Utsunomiya, JAPAN

**TWENTIETH EUROPEAN ROTORCRAFT FORUM**  
**OCTOBER 4 - 7, 1994 AMSTERDAM**

# DESIGN OF NEW GENERATION ROTOR BLADE AIRFOILS USING NAVIER-STOKES

by  
M. Nakadate and M. Obukata  
Fuji Heavy Industries, Ltd.  
Utsunomiya, JAPAN

## Abstract

A study on the design of new generation rotor blade airfoils has been carried out to develop new rotors for helicopters. Beginning by discussing the design criteria for rotor blade airfoils, aerodynamic analysis methods used in the design are outlined and design procedures in terms of analysis methods are described. State-of-the-art Navier-Stokes code was extensively used in the design procedures to satisfy the design criteria and to achieve the design goals. In the practical design, a parametric analysis on the leading edge shape is followed by an optimization of the shape and then the shape is refined to obtain the final airfoil. A two dimensional transonic wind tunnel test was conducted on the new airfoil to confirm the design. The analysis results agreed well with the wind tunnel results and it was confirmed that the airfoil achieved or exceeded the design goals.

## List of Symbols

$c$	airfoil section chord length
$C_d$	airfoil section drag coefficient
$C_l$	airfoil section lift coefficient
$C_{l_{max}}$	airfoil section maximum lift coefficient
$C_m$	airfoil section pitching moment coefficient about the quarter chord
$C_{m_0}$	airfoil section zero lift pitching moment coefficient
$C_p$	airfoil section pressure coefficient
$E, F$	inviscid flux vectors
$E_v, F_v$	viscous flux vectors
GK	Garabedian-Korn
$l/d$	airfoil section lift to drag ratio
$M$	Mach number
$M_{dd}$	airfoil section drag divergence Mach number
$M_L$	airfoil section local Mach number
NS	Navier-Stokes
$Q$	source vector
$Re$	Reynolds number based on airfoil chord length
$t$	time
$t/c$	airfoil section thickness to chord ratio
$x, y$	Cartesian coordinates

$x_{LEC}$	chord station where leading edge camber (nose droop) ends, % chord
$x_{t/cmax}$	chord station where $t/c$ is maximum, % chord
$y_{LEC}$	magnitude of leading edge camber at the leading edge, % chord
$\alpha$	airfoil section angle of attack, deg.
$\eta, \xi$	generalized curvilinear coordinates

## Introduction

Recent progress in the performance of helicopters has been so remarkable that the maximum speed of over 200 kt is not uncommon among experimental helicopters (figure 1). Such high performance owes much to the progress in aerodynamics including advanced airfoils.

Also remarkable has been the recent progress in computational fluid dynamics (CFD) and supercomputers, which makes it possible to predict airfoil performance with accuracy up to maximum lift where viscous and vortical effects prevail.

In this context, a study on the design of advanced rotor blade airfoils using state-of-the-art Navier-Stokes code has been carried out at Fuji Heavy Industries as part of the company funded research. This paper concentrates chiefly on the airfoil design study in terms of aerodynamic analysis methods. Results of the computational analyses in the design will also be compared with the results of the wind tunnel test to reinforce the validity of the Navier-Stokes code as well as to confirm the design.

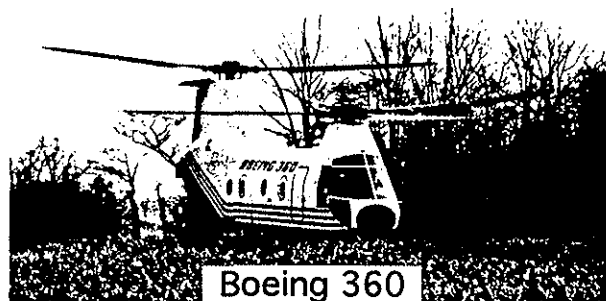
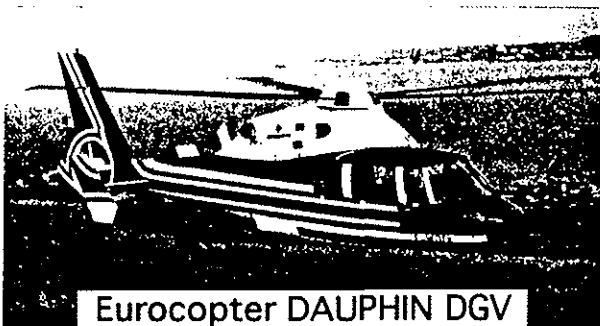


*Figure 1 Experimental High Speed Helicopters*

## Design Criteria

Before discussing the design criteria, let us review the operational conditions of rotor blades. As can be seen from figure 2, the flow around the tip of the advancing rotor blade of helicopters at high speed forward flight reaches up to transonic Mach numbers because the forward speed is added to the rotational speed. On the other hand, the dynamic pressure or the flow speed around the tip of the retreating rotor blade is low because the forward speed is subtracted from the rotational speed. Consequently the angle of attack or the local lift of the retreating rotor blade has to be high enough to balance the advancing rotor blade in high dynamic pressure, leading occasionally to local stall. Thus rotor blade airfoils need to realize high performance throughout the wide range of Mach numbers and angles of attack, that is, as referred to in various books and papers, high maximum lift at lower Mach numbers, high lift to drag ratio at mid to high subsonic Mach numbers and low drag up to transonic Mach numbers while keeping nose down pitching moment minimal.

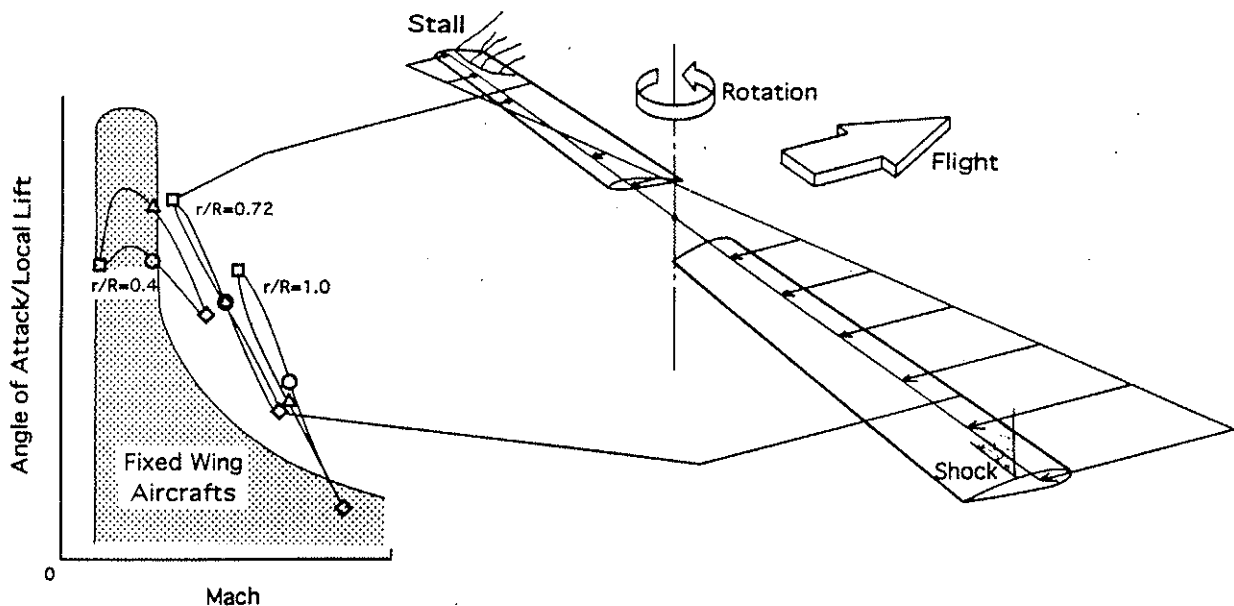


Figure 2 Operational Conditions of Rotor Blades

The following design criteria, similar to those described in references 1) through 3), were chosen for the convenience of comparison.

1. High maximum lift at 0.4 Mach
  - to delay the stall on the retreating rotor blade and reduce the vibration at high thrust.

2. High drag divergence Mach numbers
  - to reduce the drag on the advancing rotor blade and reduce the power required.
3. Low drag level at 0.6 Mach, 0.6 Cl
  - to reduce the drag on the blade and improve the hover efficiency.
4. Low zero lift nose down pitching moment at 0.6 Mach
  - to reduce the load on the blades and to the control systems.

## Analysis Methods and Design Procedures

A compressible two dimensional Navier-Stokes code was incorporated into the design procedures, which made efficient as well as accurate prediction of maximum lift possible. The following three analysis methods were used in the design. Their features are outlined below.

1. CLMAX two dimensional potential code (vortex panel method)<sup>4)</sup>
  - Calculates the flow about airfoils up to and beyond the stall.
  - The vortex panel method is coupled to a laminar boundary layer, or Curle's method<sup>5)</sup> and an integral boundary layer method developed by Nash and Hicks<sup>6)</sup>. The laminar calculation is performed along the airfoil until transition is found, and then the turbulent calculation starts. Separation is judged when the skin friction comes to zero. Free vortex sheets are used to model a wake when separation is found. An iterative procedure is employed to establish their shapes.
  - In the practical design the use of this code was restricted to the comparative evaluation of Clmax because the code estimated Clmax well qualitatively but significant discrepancy in Clmax level was also found.
  - Only 0.1 CPU minute on IBM 3090 computer.
2. Garabedian-Korn two dimensional full potential code<sup>7)</sup>
  - Calculates the flow about airfoils up to transonic Mach numbers with reasonable accuracy.
  - Based on the finite difference scheme. A conformal transformation is used for the grid generation to realize orthogonality. Viscous effects are taken into account by adding the boundary layer displacement thickness to the airfoil shape.
  - About 0.5 CPU minute on IBM 3090 computer.
  - Used to evaluate the drag divergence Mach numbers, the drag polars and the pitching moment.
3. Compressible two dimensional Navier-Stokes code
  - This code will be discussed in the next section.

Inverse design methods<sup>8)</sup>, which can be coupled to any analysis method and calculate the wing or airfoil geometry with the specified pressure distribution up to the transonic region, are useful in designing

wings or airfoils in case the desirable pressure can easily be determined. However, such methods were not used in the practical design because, unlike jet transport wings or airfoils, the design of rotor blade airfoils can not solely be concentrated on the cruise condition, which makes it difficult to establish a specific pressure distribution desirable for rotor blade airfoils.

An outline of design procedures in terms of analysis methods is shown in figure 3.

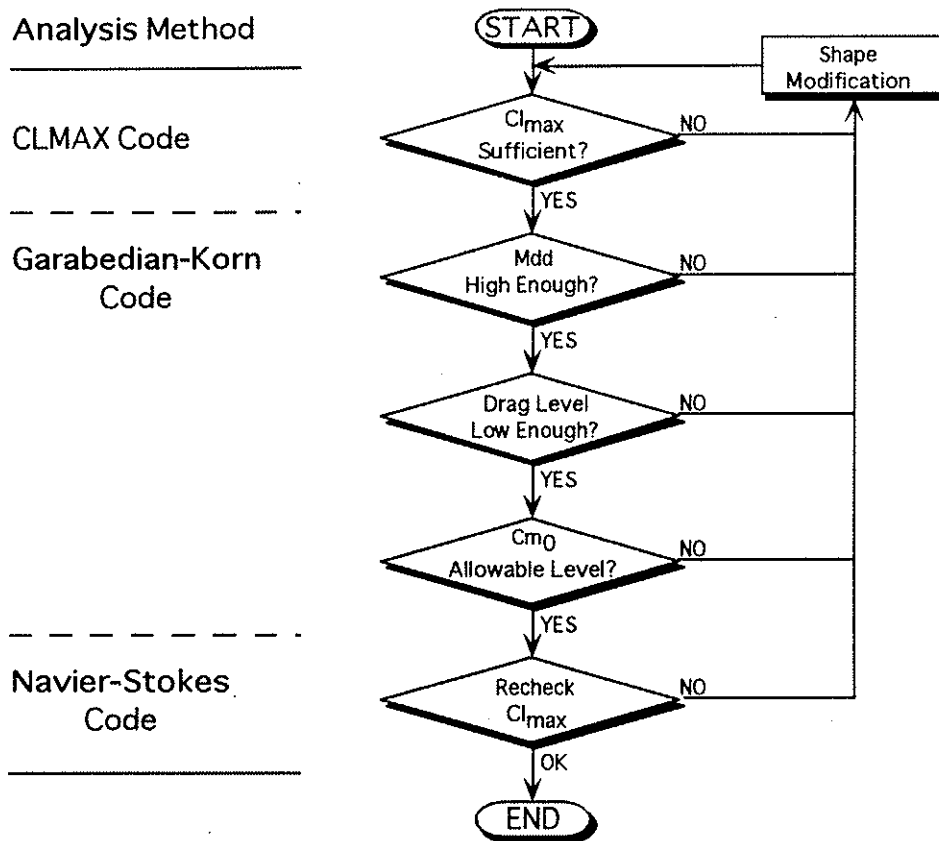


Figure 3 Design Procedures in Terms of Analysis Methods

## Navier-Stokes Code

The conservation law form of the compressible two dimensional Reynolds-averaged Navier-Stokes (RANS) equations in the Cartesian coordinates  $x$ ,  $y$  and time  $t$  is given by

$$\partial Q/\partial t + \partial E/\partial x + \partial F/\partial y = Re^{-1}(\partial E_v/\partial x + \partial F_v/\partial y) \quad (1)$$

where  $Q$  is the source vector,  $E$  and  $F$  are the inviscid flux vectors,  $E_v$  and  $F_v$  are the viscous flux vectors.

Under a thin-layer approximation, the viscous flux vector in x direction is neglected and then equation (1) simplifies to

$$\partial Q/\partial t + \partial E/\partial x + \partial F/\partial y = Re^{-1} \partial F_v/\partial y \quad (2)$$

A generalized curvilinear coordinate transformation is utilized to transform the physical domain into a rectangular computational domain. Algebraically generated "C" grid is used in the practical computation.

A third-order upwind TVD (Total Variation Diminishing) scheme<sup>9)</sup> for the space discretization and an LU-ADI (Lower-Upper Alternating Direction Implicit) factorization scheme<sup>10)</sup> for the time integration are used to obtain solutions. Spatially varying time step is also used. Consequently high speed as well as high accuracy is realized. A couple of CPU minutes on our 5 GFLOPS Fujitsu VP-2600 supercomputer.

Baldwin-Lomax algebraic turbulence model<sup>11)</sup> is employed to describe the sub-grid size turbulence effects.

Prior to the design,  $C_{lmax}$  was calculated about several airfoils using the Navier-Stokes code and compared with the wind tunnel results to check if the code can be used for the practical design. Figure 4 shows the Navier-Stokes analysis versus wind tunnel comparison. The NS results agreed well with the wind tunnel results. The difference between the analysis and the wind tunnel is small enough for the NS code to be used as a design tool when compared with the scatter of published data among wind tunnels. However, special care must be taken because some airfoils like NACA 23012 show higher  $C_{lmax}$  than the wind tunnel results. It was also found that NS analysis results in terms of  $C_{lmax}$  depend sometimes upon the computational grid, about which further investigation is needed.

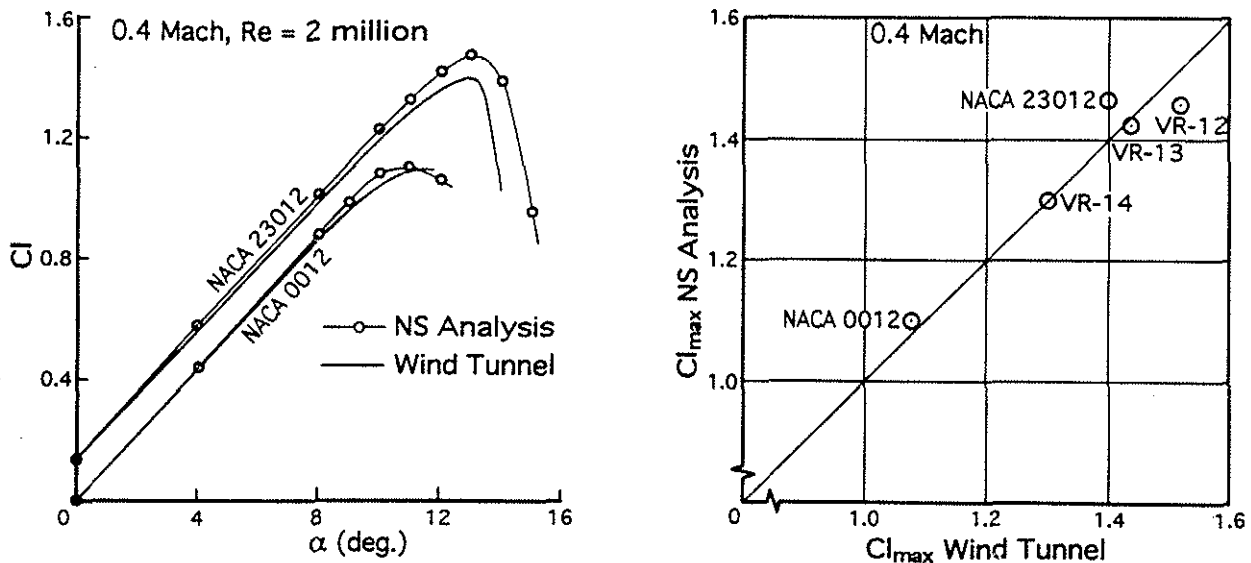


Figure 4 Analysis versus Wind Tunnel Comparison about  $C_{lmax}$



## Design Goals

In accordance with the design criteria, the following were selected as the practical design goals to realize the comparable performance to that of the third generation rotor blade airfoils like VR-12 and VR-13<sup>2)</sup> of Boeing.

- |  |            |        |       |
|--|------------|--------|-------|
| 1. Maximum lift at 0.4 Mach :              | $C_{lmax}$ | $\geq$ | 1.5   |
| 2. Zero lift drag divergence Mach number : | $M_{dd}$   | $\geq$ | 0.80  |
| 3. Drag level at 0.6 Mach and 0.6 $C_l$ :  | $C_d$      | $\leq$ | 0.010 |
| 4. Zero lift pitching moment at 0.6 Mach : | $ C_{m0} $ | $\leq$ | 0.015 |

## Airfoil Design

First of all, the thickness of 10 % chord, as a medial value of VR-12 and VR-13, was selected for the airfoil being designed.

In practice, the design was carried out along the following sequence, taking the fact into consideration that the maximum lift of airfoils depends much upon the leading edge shape, especially upon the leading edge thickness and camber.

### 1. Parametric analysis on the leading edge shape

- A symmetric high lift transonic airfoil, originally obtained in the course of designing horizontal tail airfoils for jet transports, was selected for the reference airfoil of the parametric analysis.
- The effects of the leading edge thickness and the leading edge camber (nose droop) on airfoil characteristics were analyzed throughout the wide range of shapes.
- The chord station of maximum thickness was used to represent the leading edge thickness.
- The chord station where the leading edge camber ends as well as the magnitude of the leading edge camber at the leading edge were used to represent the leading edge camber.
- Zero lift drag level at 0.8 Mach was used to represent the drag near the drag divergence Mach number.
- In addition to the analyzed drag level, the local Mach peak around the leading edge, upon which the drag level is dependent, was also checked if it is lower than 1.2, or FHI (Fuji Heavy Industries) criterion.

Figures 5-1 through 5-3 show the results from the parametric analysis.



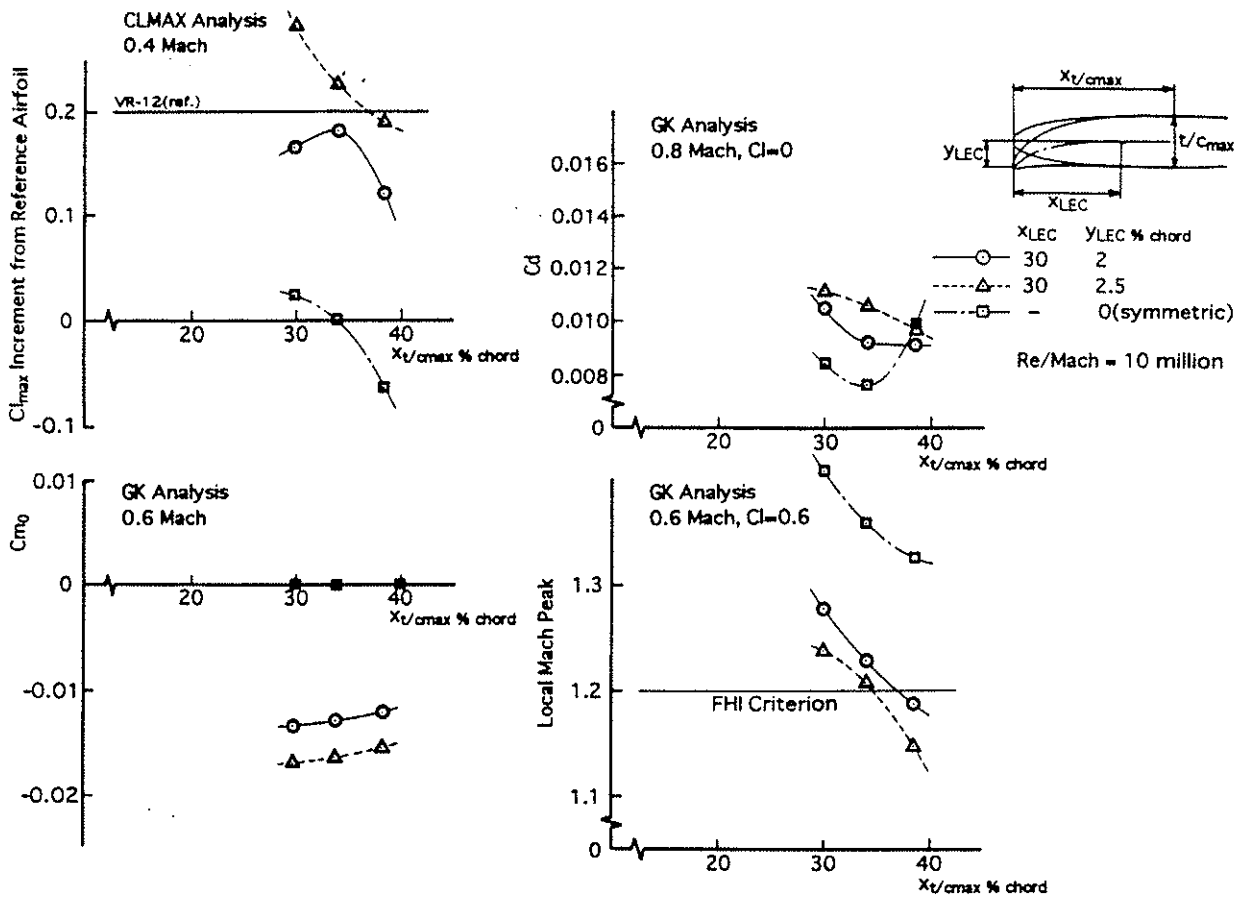


Figure 5-1 Parametric Analysis on the Leading Edge Shape(1/3)

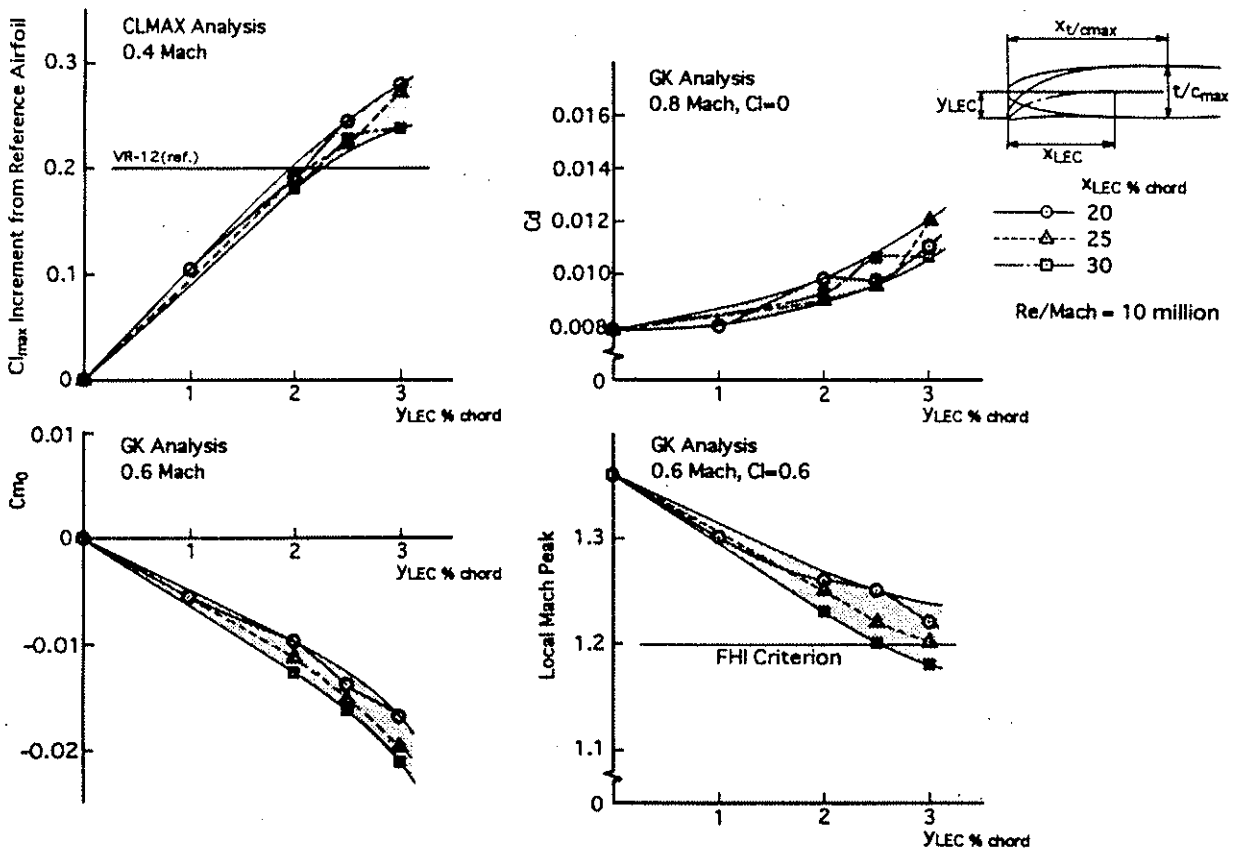


Figure 5-2 Parametric Analysis on the Leading Edge Shape(2/3)

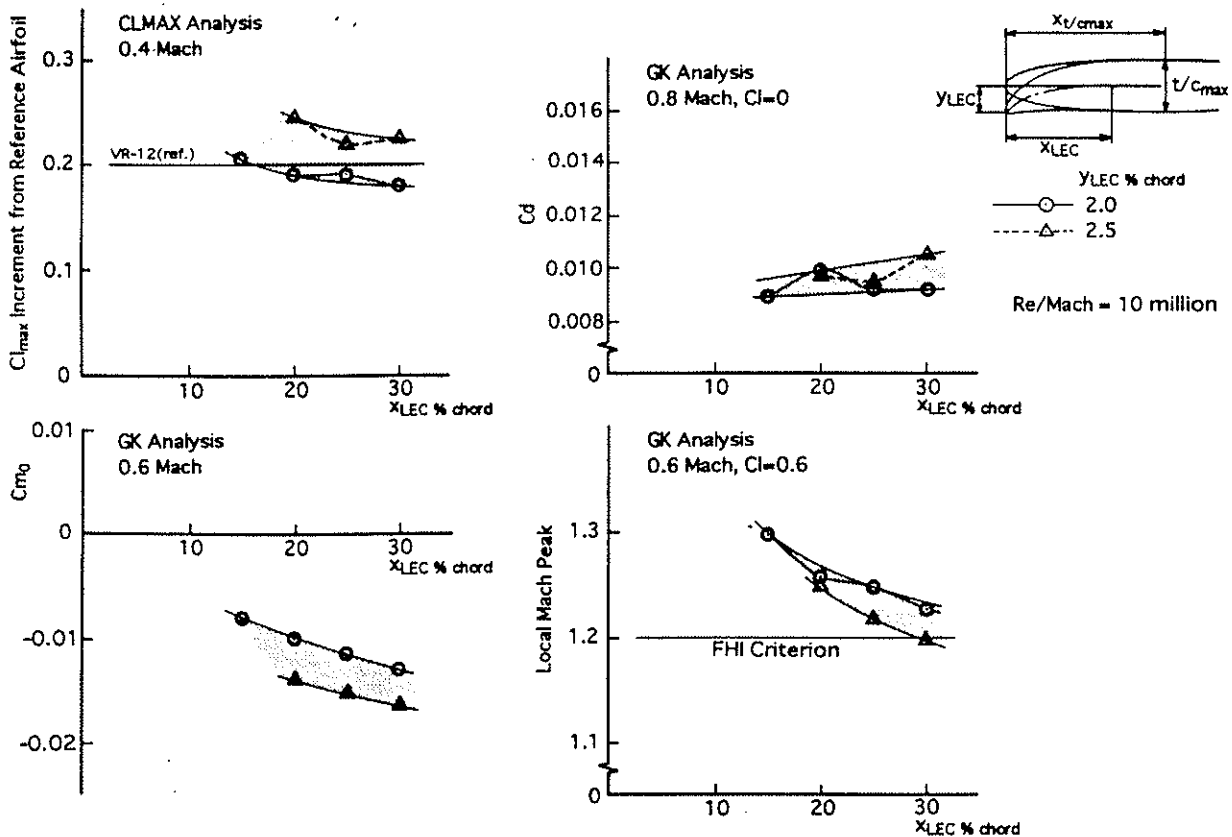


Figure 5-3 Parametric Analysis on the Leading Edge Shape(3/3)

## 2. Optimization of the leading edge shape

- An optimal combination of the leading edge thickness and the leading edge camber was selected from the results of the parametric study.
- The chord station of maximum thickness is slightly larger than 35% chord, the chord station where leading edge camber ends is around 25% chord and the magnitude of the leading edge camber at the leading edge is around 2.5 % chord.

## 3. Refining the shape

- The maximum lift about the optimal combination was checked again using Navier-Stokes code and the shape around the leading edge was refined to realize much higher maximum lift and much lower drag level by relaxing the leading edge pressure or local Mach peak (figure 6).
- Pressure distribution especially the location and strength of shock about the mid chord was also checked and the curvature was further smoothed.
- Finally, the pressure distribution around the trailing edge was checked and a moderate trailing edge angle was selected to realize good pressure recovery.

4. Check on overall and off-design characteristics

- The drag polars and pitching moment were also checked from lower Mach numbers up to transonic Mach numbers and from low angles of attack up to the stall.

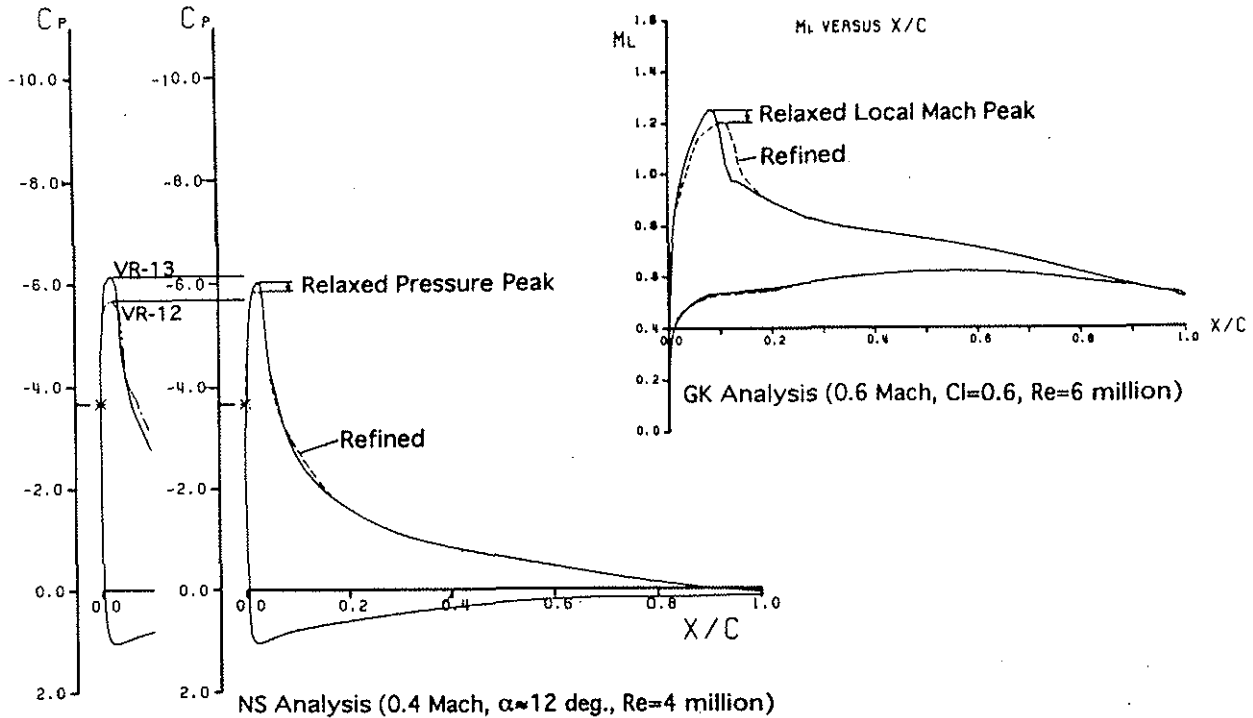


Figure 6 Relaxation of Leading Edge Pressure/Local Mach Peak

## Results of the Design

Figure 7 shows the airfoil designed above and figure 8 shows the  $301 \times 51$  ( $\xi \times \eta$ ) points computational grid of the airfoil used for the Navier-Stokes analyses. Figure 9 shows the examples of the analyzed pressure contours and pressure distribution. The airfoil has the designation of U896H-10 and the thickness of 10 % chord. The shape of the airfoil is symmetric except for the optimized thickness and camber around the leading edge. By multiplying the y coordinates by constants, a series of U896H family airfoils with various thickness can easily be obtained.

Figure 10 shows the analysis versus wind tunnel results comparison of maximum lift and drag divergence Mach number. The analysis results agreed well with the wind tunnel results and U896H-10 airfoil exhibited the high performance as predicted.

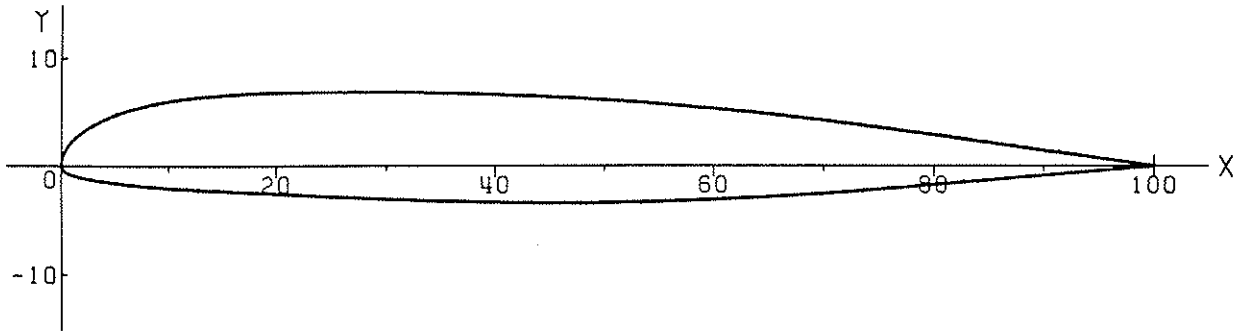


Figure 7 U896H-10 Airfoil

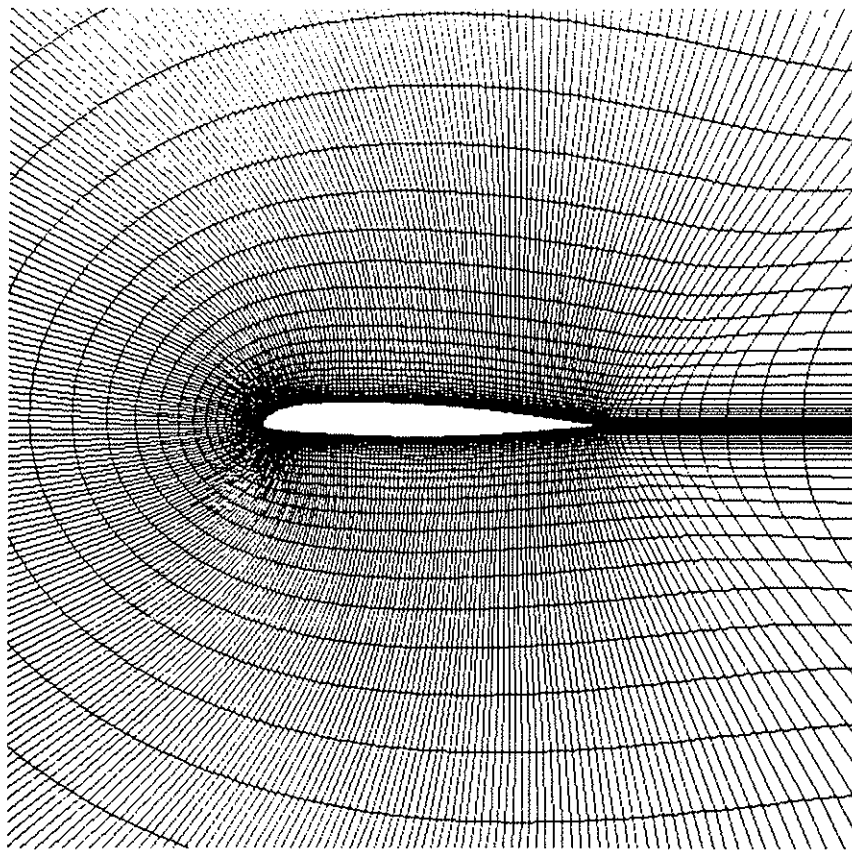
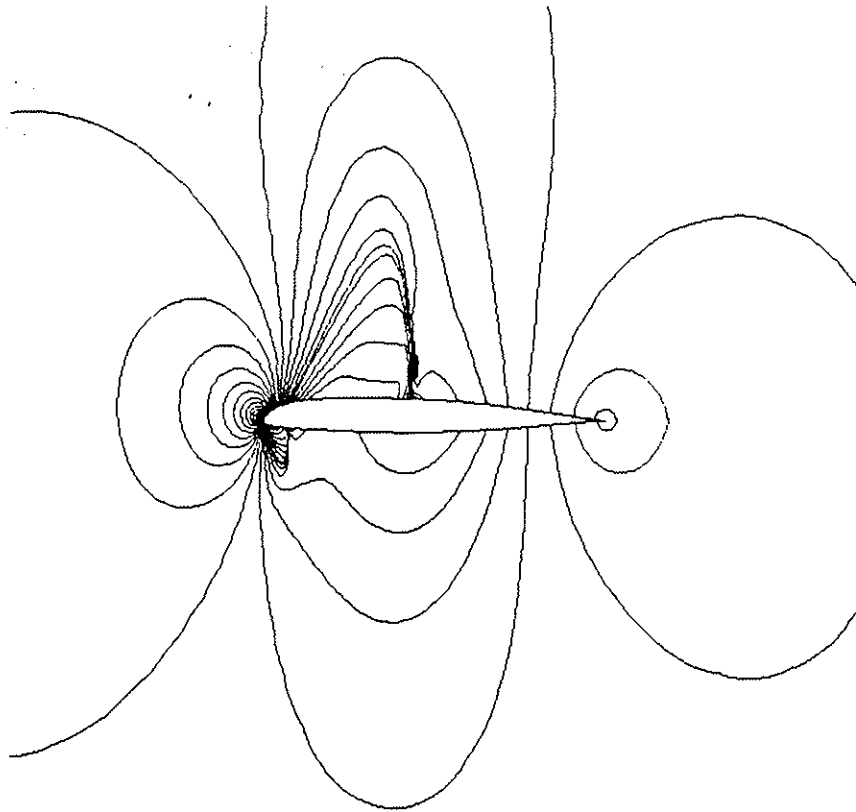
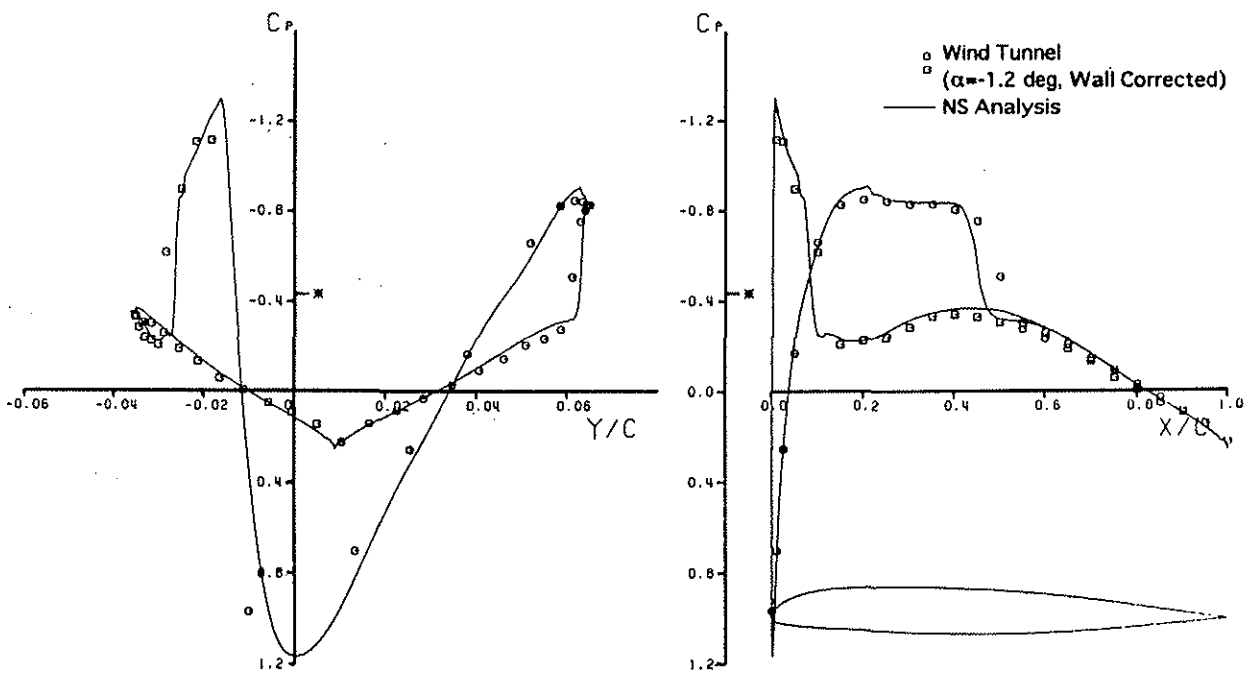


Figure 8 U896H-10 301x51 ( $\xi \times \eta$ ) Points Computational Grid



Pressure Contours



Pressure Distribution

Figure 9 U896H-10 Navier-Stokes Results ( $M=0.8$ ,  $\alpha=-1$  deg.)

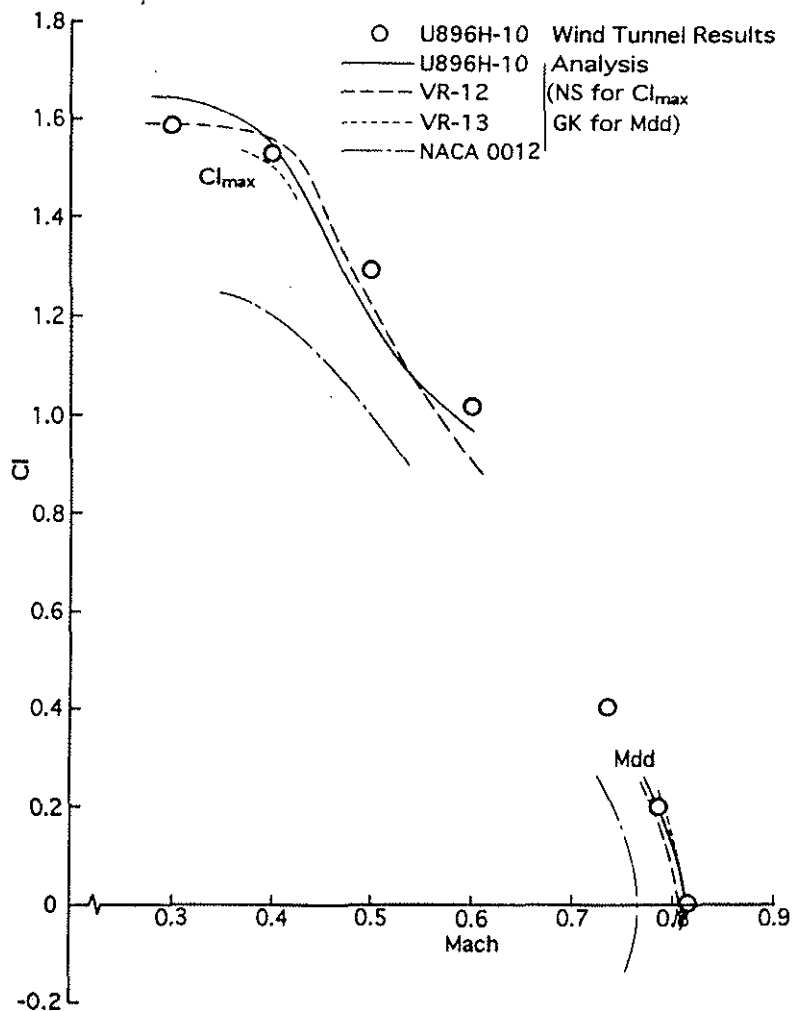


Figure 10 Analysis versus Wind Tunnel Comparison

## Concluding Remarks

- The wind tunnel results confirmed that the designed airfoil achieved or exceeded the design goals. Among new generation rotor blade airfoils came new U896H series airfoils. Figure 11 shows the  $C_{l_{max}}$  versus drag divergence Mach number of the airfoil compared with other airfoils.
- By using state-of-the-art Navier-Stokes code, the performance of airfoils including maximum lift was predicted with considerable accuracy, which made the design of advanced rotor blade airfoils much easier and more efficient.
- To realize much higher performance, the design in the unsteady condition as well as in the three dimensional condition is required.

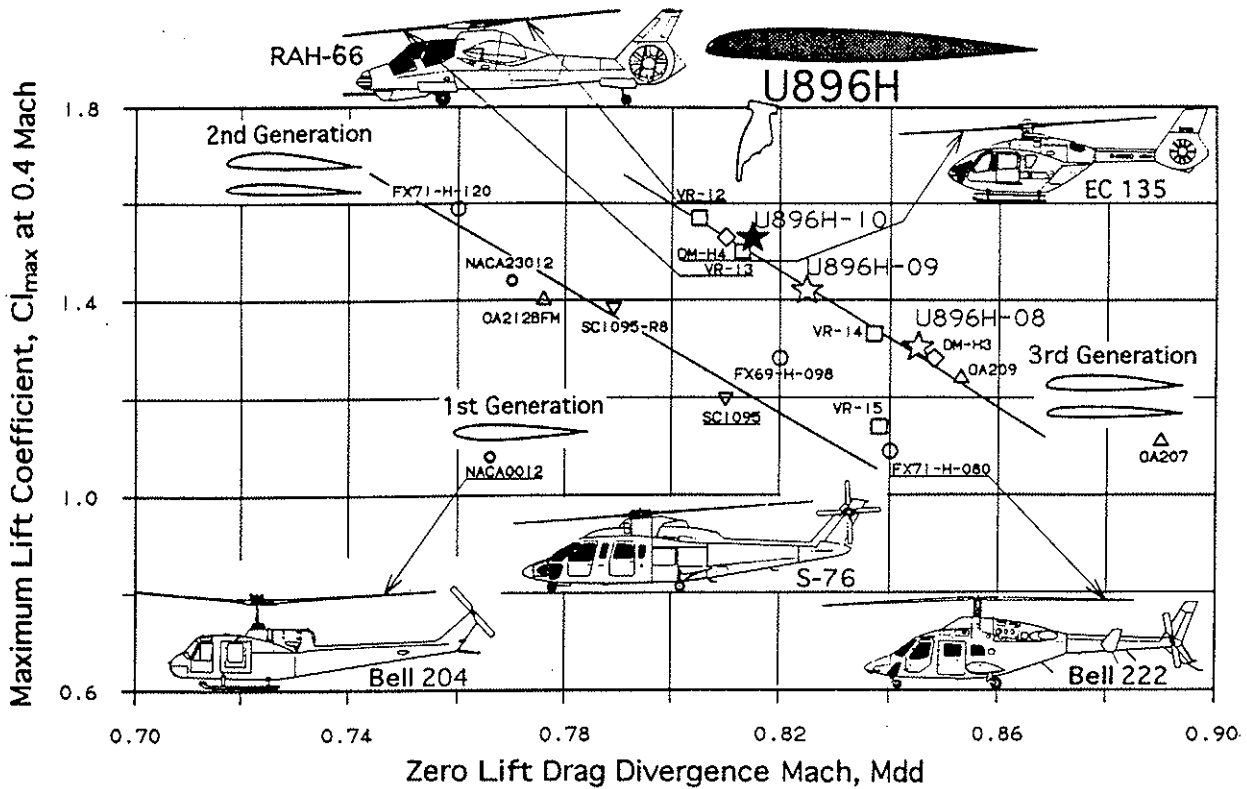


Figure 11 Rotor Blade Airfoils Comparison

## References

- 1) J.J.Thibert and J.M.Pouradier, Design and Test of an Helicopter Rotor Blade with Evolutive Profile., ICAS-80-10.3, 1980
- 2) M.A.McVeigh and F.J.McHugh, Recent Advances in Rotor Technology at Boeing Vertol., paper presented at the 38th Annual Forum of the American Helicopter Society, 1982
- 3) K.H.Horstmann, H.Koster and G.Polz, Development of New Airfoil Sections for Helicopter Rotor Blades., paper presented at the 8th European Rotorcraft Forum, 1982
- 4) B.Maskew and F.A.Dvorak, Investigation of Separation Models for the Prediction of  $Cl_{max}$ ., paper presented at the 33rd Annual Forum of the American Helicopter Society, 1977
- 5) H.Curle, A Two-Parameter Method for Calculating the Two-Dimensional Incompressible Laminar Boundary Layer., Journal of the Royal Aeronautical Society, Vol.71, 1967



- 6) J.F.Nash and J.G.Hicks, An Integral Method Including the Effect of Upstream History on the Turbulent Shear Stress., Computation of Turbulent Boundary Layers - 1968 AFOSR-IFP Stanford Conference, Vol. 1, Stanford University Department of Mechanical Engineering, 1969
- 7) F.Bauer, P.Garabedian, D.Korn and A.Jameson, Supercritical Wing Sections II., Springer-Verlag, Berlin, Heidelberg, New York, 1975
- 8) S.Takanashi, An Iterative Procedure for Three-Dimensional Transonic Wing Design by the Integral Equation Method., AIAA Paper 84-2155, 1984
- 9) S.R.Chakravarthy and S.Osher, A New Class of High Accuracy TVD Scheme for Hyperbolic Conservation Laws., AIAA Paper 85-0363, 1985
- 10) S.Obayashi, K.Matsushima, K.Fujii and K.Kuwahara, Improvements in Efficiency and Reliability for Navier-Stokes Computation Using the LU-ADI Factorization Algorithm., AIAA Paper 86-0338, 1986
- 11) B.S.Baldwin and H.Lomax, Thin Layer Approximation and Algebraic Model for Separated Turbulent Flows., AIAA Paper 78-0257, 1978